

# **A Systematic Representation Method of the Odometry Uncertainty of Mobile Robots**

Nakju Lett Doh<sup>†</sup> and Wan Kyun Chung<sup>‡</sup>

<sup>†</sup> Graduate student, Department of Mechanical Engineering, POSTECH

<sup>‡</sup> Professor, Department of Mechanical Engineering, POSTECH

Please address all the correspondence to Prof. Wan Kyun Chung (wkchung@postech.ac.kr)

<sup>†, ‡</sup> Robotics & Bio-Mechatronics Lab., Department of Mechanical Engineering,

Pohang University of Science & Technology (POSTECH)

San-31, Hyoja-Dong, Pohang, 790-784, KOREA

E-mail: {nakji,wkchung}@postech.ac.kr

Fax: +82-54-279-5899, Tel: +82-54-279-2844

---

## **Abstract**

A covariance matrix is a tool that expresses the odometry uncertainty of mobile robots. The covariance matrix is a key factor in various localization algorithms such as the Kalman filter or topological matching. However, it is not easy to acquire an accurate covariance matrix because the real states of robots are not known. Till now, few results on estimating the covariance matrix have been reported. Also, those are not validated by experiments or do not reflect the real phenomena. In this paper, we propose a novel method which approximates the covariance matrix in a physically reasonable way. Extensive experiments validate that our method yields a covariance matrix which is accurate enough for practical uses.

## **Keywords**

Odometry uncertainty, relative localization, covariance matrix, generalized Voronoi graph, odometry calibration, mobile robot.

# A Systematic Representation Method of the Odometry Uncertainty of Mobile Robots

Nakju Lett Doh      Wan Kyun Chung

Robotics & Bio-Mechatronics Lab., Mechanical Engineering,

Pohang University of Science & Technology (POSTECH), Pohang, KOREA

Tel : 82-54-279-2844 ; Fax : 82-54-279-5899; E-mail : {nakji,wkchung}@postech.ac.kr

## Abstract

*A covariance matrix is a tool that expresses the odometry uncertainty of mobile robots. The covariance matrix is a key factor in various localization algorithms such as the Kalman filter or topological matching. However, it is not easy to acquire an accurate covariance matrix because the real states of robots are not known. Till now, few results on estimating the covariance matrix have been reported. Also, those are not validated by experiments or do not reflect the real phenomena. In this paper, we propose a novel method which approximates the covariance matrix in a physically reasonable way. Extensive experiments validate that our method yields a covariance matrix which is accurate enough for practical uses.*

## keywords

Odometry uncertainty, relative localization, covariance matrix, generalized Voronoi graph, odometry calibration, mobile robot.

## 1 Introduction

A position estimator using odometry suffers from systematic and non-systematic errors [1]. The systematic errors tend to be the functions of the system caused by the wheel diameter difference, inaccurate wheel base length, etc. The non-systematic errors are independent of the robot, and they are caused by wheel slippage, an imperfect floor surface, etc.

The systematic errors can be predicted and effectively compensated for as in [1,2]. The non-systematic errors, however, cannot be compensated for because they are random errors. Thus, researchers have adopted the Gaussian probability to express the non-systematic error. Sebastian Thrun, *et al.* [3] showed that the Gaussian probability yields an error bound of odometry which looks like a banana (Fig. 1(a)). However, there is no model which can represent this banana shape. Thus, researchers [4–8] have used a covariance matrix whose ellipse can approximate the banana-like shape (Fig. 1(b)).

However, a precise knowledge of the covariance matrix is difficult to obtain because no information on the ground truth can be provided. Thus some researchers have simply assumed the covariance matrix to be a multiple of travel distance and a constant whose value is intuitively selected [6,7]. Wang [4] proposed an approximation method of the covariance matrix, but his approach is valid only in simulation. Also, Chong [5], Bengtsson [8], Martinelli [9], and Kelly [10] suggested covariance estimation methods, but there techniques have not been verified via extensive experiments.

In our previous paper [11], we suggested an empirical method of covariance matrix estimation based



Figure 1: If a robot follows a straight line, an error bound of odometry will look like a banana as in (a). To approximate this banana shape, researchers have used a covariance matrix whose ellipse covers the banana shape as in (b).

on the PC-method [2]. However, the previous method did not consider the covariance matrix in the robot's heading angle. As a result, an estimated covariance matrix yields an error ellipse whose major axes are aligned with the world coordinates. This does not reflect the real phenomena.

For example, a robot which moved linearly at a  $45^\circ$  angle relative to the coordinate system as in Fig. 2 would have a real error bound like the dotted ellipse. However, our previous method will yield an error ellipse whose major axes are aligned with the world coordinate. To cover the real error bound without axes rotation, the previous method intentionally enlarged the size of the ellipse. In other words, it produced an overestimated covariance matrix.

In this paper, we propose a new covariance estimation method which also considers the covariance of the robot's heading angle. This new method precisely estimates the covariance matrix whose axes are not aligned with the world coordinate and thus reflects the real phenomena more closely.

The basic idea of this method is as follows: A robot, whose systematic errors are fully compensated for,

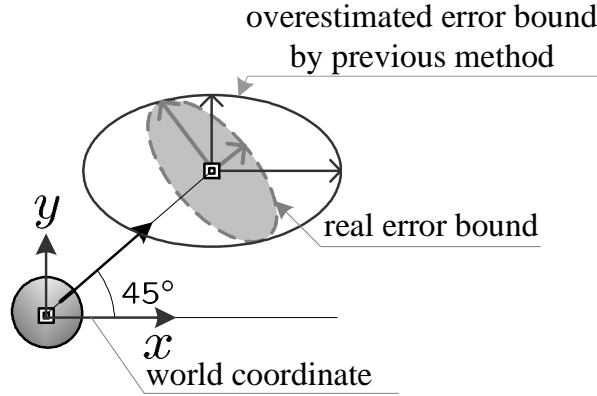


Figure 2: A robot moved a straight line rotated by  $45^\circ$ . The real error bound, then, will be like the dotted ellipse but our previous method will yield an overestimated error bound whose axes are aligned with the world coordinate.

navigates the same path twice. There are, then, two odometry paths that do not overlap each other due to non-systematic errors. Thus a set of values which makes the two odometry paths coincide is the non-systematic errors. Once these values are acquired, we can calculate expectation values of the non-systematic errors. The covariance matrix can be estimated by using these expectation values.

We believe that the proposed method can be used for all mobile bases. However, in this paper, we apply the proposed method to synchro and differential drive robots whose odometry models are given. Recall that a synchro-drive robot has three or four wheels that translate and rotate in a synchronous manner. Its motion is accomplished by two control motors: one for translation and the other for rotation. The differential drive robot has two control motors that can be controlled independently.

For validation purposes, two robots (a synchro-drive robot and a differential drive robot) were ran 200 times along 4 different paths. These extensive experimental results validate that the covariance matrix acquired by the proposed method is accurate enough for practical use (less than 9 % offset from the

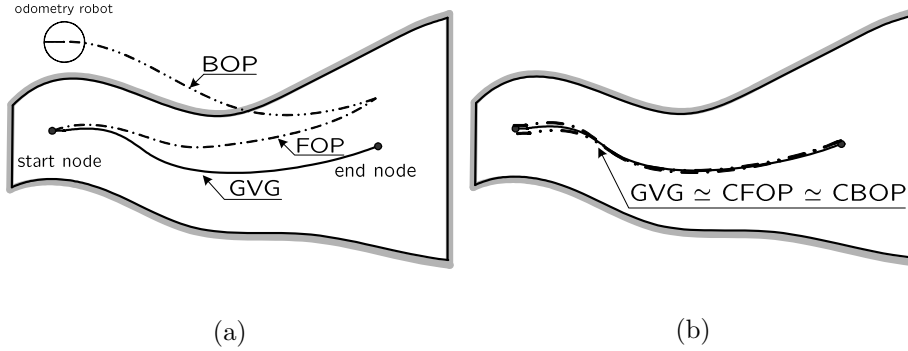


Figure 3: Schematic explanation of the PC-method. (a) is a plot before correction and (b) is a plot after correction.

ideal value).

This paper is organized as follows: In section 2, the PC-method is briefly introduced. The method of covariance matrix estimation is explained in section 3. The experimental results are shown in sections 4 and 5 for the synchro and the differential drive robots. A conclusion then follows.

## 2 Description of the PC-method

The PC-method [2] is based on the idea that a sensor-based navigation through the Generalized Voronoi Graph (or GVG) bounds the absolute error while odometry does not. Recall that the GVG [12] is a set of points whose edges and nodes are equidistant to two or more objects. Thus, if a robot navigates the GVG twice, once forward and then backward, two different odometry paths are generated, but along the same path on the GVG in the real world.

The sensor and control errors can be assumed to be small enough to be ignored during the GVG navigation. Then if the two different odometry paths are compensated for using *a true odometry error*

*model* and *real error parameters*, the compensated paths will overlap. Thus, once we have the two different odometry paths and the true odometry error model, we can estimate the error parameters which minimize the position errors between the two paths.

The estimation procedure of the PC-method is given below with a schematic explanation in Fig. 3.

---

1. Navigate a GVG path from a start node to an end node. The start and end nodes can be chosen arbitrarily as long as the length between the two nodes is long “enough” for parameter estimation. This first set of data is denoted as a Forward Odometry Path (FOP).
  2. Turn the robot  $180^\circ$  and navigate from the end node to the start node. We will denote this odometry data as a Backward Odometry Path (BOP).
  3. Take an initial guess of the error parameters which produce a Corrected FOP (CFOP) and a Corrected BOP (CBOP) using the given error model.
  4. Starting with this initial guess, perform optimizations to find the error parameters that minimize the position error between the CFOP and the CBOP.
- 

### 3 Covariance estimation method

In this section, we propose a covariance estimation technique based on the PC-method. This new approach calculates the covariance matrix of a corrected odometry (an odometry calibrated by the odometry error model and the error parameters) in a natural manner.

If the systematic errors are fully compensated for, then encoder values are the sum of the real signals

and the non-systematic errors. These values of the synchro-drive robot are

$$\Delta D(k) = \Delta D_{real}(k) + \epsilon_D(k), \quad (1)$$

$$\Delta \Theta(k) = \Delta \Theta_{real}(k) + \epsilon_{\Theta}(k),$$

where  $(\Delta D(k), \Delta \Theta(k)), (\Delta D_{real}(k), \Delta \Theta_{real}(k))$  and  $(\epsilon_D(k), \epsilon_{\Theta}(k))$  are the stepwise translation/rotation, the real stepwise translation/rotation and translational/rotational non-systematic errors at the  $k$ -th step.

Similarly, the encoder values of the differential drive robot are

$$\delta r(k) = \delta r_{real}(k) + \epsilon_r(k), \quad (2)$$

$$\delta l(k) = \delta l_{real}(k) + \epsilon_l(k),$$

where  $(\delta r(k), \delta l(k)), (\delta r_{real}, \delta l_{real})$  and  $(\epsilon_r(k), \epsilon_l(k))$  are a stepwise increase, the real increase and the non-systematic errors of the right/left wheels at the  $k$ -th step.

The non-systematic errors can be estimated from the corrected forward odometry path (CFOP) and the corrected backward odometry path (CBOP). If the CFOP exactly matches the GVG, deviations between the CFOP and the CBOP are induced by the non-systematic errors. Thus the non-systematic errors can be estimated by calculating  $\epsilon_{(\cdot)}$  that makes a CBOP point overlap with its matching CFOP position as shown in Fig. 4.

Using these  $\epsilon_{(\cdot)}$ , sample variances of stepwise translation and rotation can be calculated. The sample variances of the synchro drive robot are

$$\begin{aligned} \sigma_{\Delta D}^2 &= \frac{1}{n-1} \sum_{i=1}^n (\epsilon_D(i) - \bar{\epsilon}_D)^2, \\ \sigma_{\Delta \Theta}^2 &= \frac{1}{n-1} \sum_{i=1}^n (\epsilon_{\Theta}(i) - \bar{\epsilon}_{\Theta})^2, \end{aligned} \quad (3)$$

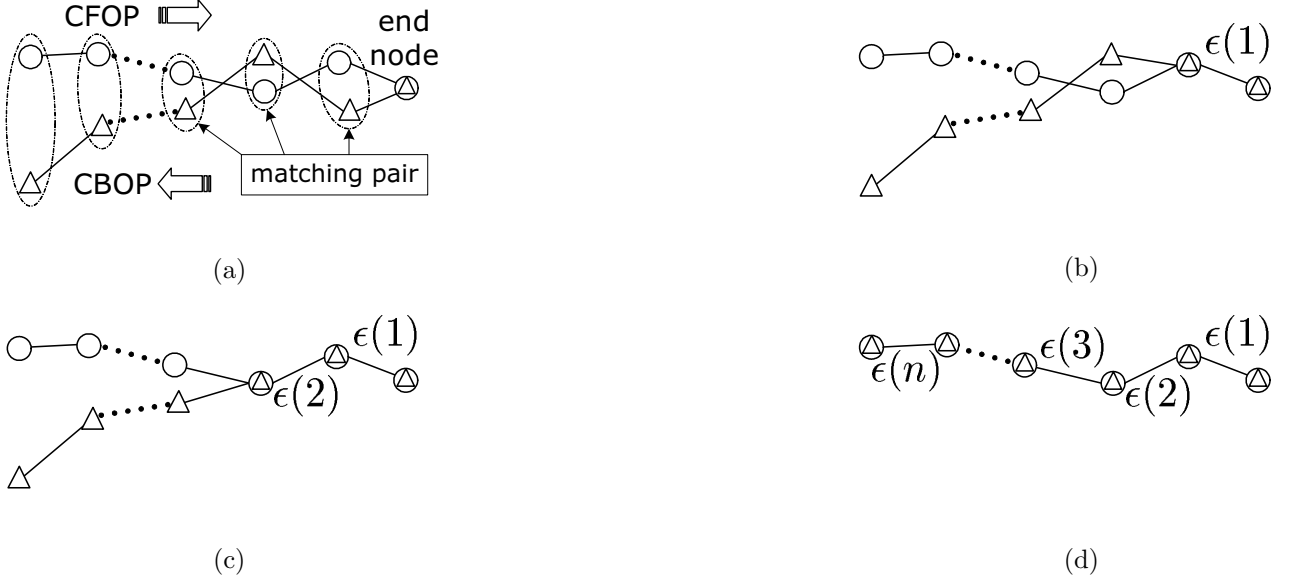


Figure 4: Method of approximating the non-systematic errors: (a) The CFOP/CBOP do not perfectly overlap even after the systematic error compensation. (b)  $\epsilon_{(\cdot)}(1)$  can be found which changes the first CBOP point into its matching CFOP point. This procedure can be applied to succeeding matching pairs as in (c) and (d).

where  $n$  is the number of samples in the CFOP and  $\bar{\epsilon}_{(\cdot)} = \frac{1}{n} \sum_{i=1}^n \epsilon_{(\cdot)}(i)$ .

For differential drive robots,  $\Delta D(k) = \frac{\delta r(k) + \delta l(k)}{2}$  and  $\Delta \Theta(k) = \frac{\delta r(k) - \delta l(k)}{b}$  where  $b$  is the wheel base length. Thus the variances of stepwise translation and rotation are

$$\begin{aligned} \sigma_{\Delta D}^2 &= \frac{1}{4n} \left\{ \sum_{i=1}^n (\epsilon_r(i) - \bar{\epsilon}_r)^2 + \sum_{i=1}^n (\epsilon_l(i) - \bar{\epsilon}_l)^2 \right\}, \\ \sigma_{\Delta \Theta}^2 &= \frac{1}{b^2 n} \left\{ \sum_{i=1}^n (\epsilon_r(i) - \bar{\epsilon}_r)^2 + \sum_{i=1}^n (\epsilon_l(i) - \bar{\epsilon}_l)^2 \right\}. \end{aligned} \quad (4)$$

Among the state  $(x, y, \theta)$ , the variance of the heading angle (denote it  $\sigma_{\theta}^2$ ) will be derived first. The kinematic equation of  $\theta$  is

$$\theta(k+1) = \theta(k) + \Delta \Theta(k). \quad (5)$$

From (5),  $\sigma_\theta^2$  can be calculated as

$$\begin{aligned}\sigma_\theta^2(k+1) &= \sigma_\theta^2(k) + \text{var}[\Delta\Theta(k)] + \text{cov}[\theta(k), \Delta\Theta(k)] + \text{cov}[\Delta\Theta(k), \theta(k)] \\ &= \sigma_\theta^2(k) + \text{var}[\Delta\Theta(k)],\end{aligned}\tag{6}$$

because  $\theta(k)$  and  $\Delta\Theta(k)$  are independent [4]. Here  $\text{var}[a]$  represents the variance of  $a$ , and  $\text{cov}[a, b]$  is the covariance between  $a$  and  $b$ . The  $\text{var}[\Delta\Theta(k)]$  can be given as

$$\text{var}[\Delta\Theta(k)] = \frac{|\Delta\Theta(k)|}{\overline{\Delta\Theta}} \sigma_{\Delta\Theta}^2,\tag{7}$$

where  $\overline{\Delta\Theta} = \frac{1}{n} \sum_{i=1}^n \Delta\Theta(k)$ . Note that  $\sigma_{\Delta\Theta}^2$  is multiplied by  $\frac{|\Delta\Theta(k)|}{\overline{\Delta\Theta}}$ , because  $\sigma_{\Delta\Theta}^2$  is the variance during  $\overline{\Delta\Theta}$ .

To find variances of  $(x, y)$ , we write the kinematic equation as

$$\begin{bmatrix} x(k+1) \\ y(k+1) \end{bmatrix} = \begin{bmatrix} x(k) \\ y(k) \end{bmatrix} + \begin{bmatrix} \Delta D(k) \cos(\theta(k) + \frac{\Delta\Theta(k)}{2}) \\ \Delta D(k) \sin(\theta(k) + \frac{\Delta\Theta(k)}{2}) \end{bmatrix} \equiv \begin{bmatrix} x(k) \\ y(k) \end{bmatrix} + \begin{bmatrix} u_x(k) \\ u_y(k) \end{bmatrix}\tag{8}$$

A covariance matrix of  $(x(k), y(k))^T$  is defined as

$$\mathbf{P}(k) = \text{cov}((x(k), y(k))^T) = \begin{bmatrix} \sigma_x^2 & \sigma_{xy} \\ \sigma_{xy} & \sigma_y^2 \end{bmatrix},\tag{9}$$

where  $\sigma_{ab}$  denotes the covariance of  $a$  and  $b$ . The covariance matrix of  $(u_x(k), u_y(k))^T$  is

$$\mathbf{U}(k) = \text{cov}((u_x(k), u_y(k))^T) = \begin{bmatrix} \sigma_{u_x}^2 & \sigma_{u_x u_y} \\ \sigma_{u_x u_y} & \sigma_{u_y}^2 \end{bmatrix}.\tag{10}$$

Referring to [13], these values can be calculated as

$$\begin{pmatrix} \sigma_{u_x}^2 \\ \sigma_{u_x u_y} \\ \sigma_{u_y}^2 \end{pmatrix} = \begin{pmatrix} \Delta D^2(k) \sigma_\xi^2(k) \sin^2 \xi(k) + \sigma_{\Delta D}^2 \cos^2 \xi(k) \\ (\sigma_{\Delta D}^2 - \Delta D^2(k) \sigma_\xi^2(k)) \sin \xi(k) \cos \xi(k) \\ \Delta D^2(k) \sigma_\xi^2(k) \cos^2 \xi(k) + \sigma_{\Delta D}^2 \sin^2 \xi(k) \end{pmatrix},\tag{11}$$

where  $\xi(k) = \theta(k) + \frac{\Delta\Theta(k)}{2}$  and  $\sigma_\xi^2(k) = \sigma_\theta^2(k) + \frac{|\Delta\Theta(k)| \sigma_{\Delta\Theta}^2}{4}$ .

Now, the covariance matrix can be updated as

$$\begin{aligned} \mathbf{P}(k+1) &= \mathbf{P}(k) + \mathbf{U}(k) + \text{cov}(\mathbf{P}(k), \mathbf{U}(k)) + \text{cov}(\mathbf{U}(k), \mathbf{P}(k)) \\ &= \mathbf{P}(k) + \mathbf{U}(k), \end{aligned} \tag{12}$$

because  $(x(k), y(k))^T$  and  $(u_x(k), u_y(k))^T$  are independent. As noted by [5], (12) is an inconsistent model. In other words, if the covariance is propagated in different time steps for the same path, it yields different results. This can be solved by updating (12) for every  $\overline{\Delta D} = \frac{1}{n} \sum_{i=1}^n \Delta D(i)$ .

Three remarks should be made here. First, the covariance matrix is overestimated in a rugged environment (Fig. 5) because, in a rugged place, the FOP and the BOP are likely to depart from the real GVG because of the limited sensor and control ability. This method, therefore, is recommended only for smooth environments for accurate covariance matrix estimation. Second, it is important to precisely calibrate the systematic error before calculating the covariance matrix. If large amounts of systematic errors remain, the CFOP and CBOP are mainly affected by these systematic errors (Fig. 6). Use of an inadequately calibrated CFOP and CBOP will yield a highly overestimated covariance matrix. We, therefore, recommend a precise calibration of the systematic errors. Third, we prove that the covariance matrix is positive semi-definite in appendix A.

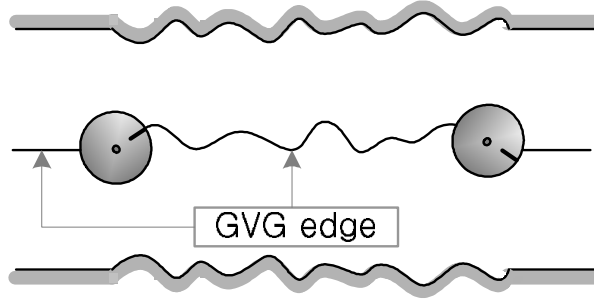


Figure 5: Typical shape of rugged environments.

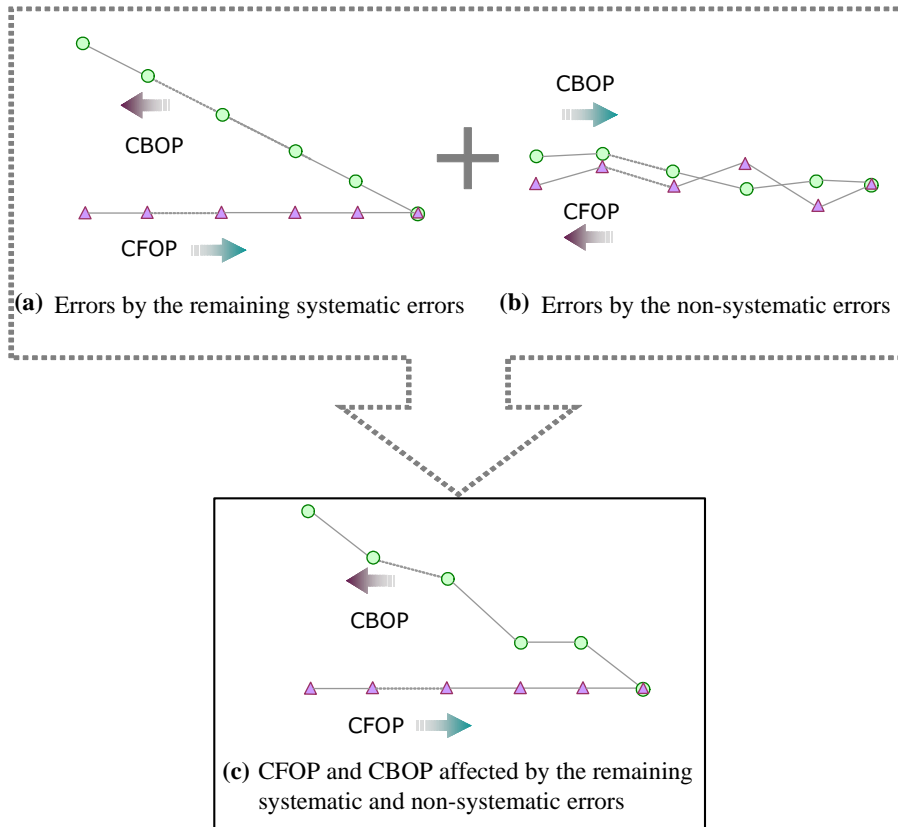


Figure 6: Large uncompensated systematic errors affect the CFOP and CBOP strongly.

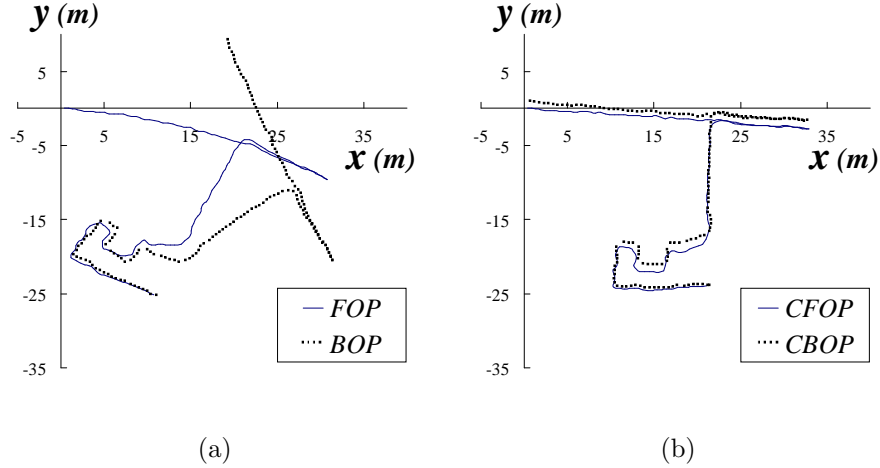


Figure 7: Forward and backward odometry paths for the error parameters estimation of the synchro-drive robot. (a) is the FOP/BOP and (b) is the CFOP/CBOP.

#### 4 Experiment 1: synchro-drive robot

The proposed method was applied to a synchro-drive robot to validate the performance of the covariance matrix estimation.

We ran the robot through a  $94.4m$  long GVG path (Fig. 7) to get the forward odometry path (FOP)/the backward odometry path (BOP) and the corrected FOP (CFOP)/the corrected BOP (CBOP).

To verify that the systematic errors are compensated for, the robot was set to yield two sets of odometry data. One is the raw odometry data and the other is the corrected odometry whose systematic errors are compensated for. The robot, then, navigated  $177.2m$ , returning to the starting point. The speed of the robot,  $0.13m/s$ , was intentionally kept low to minimize non-systematic errors. Two maps from the raw odometry and the corrected odometry are shown in Fig. 8.

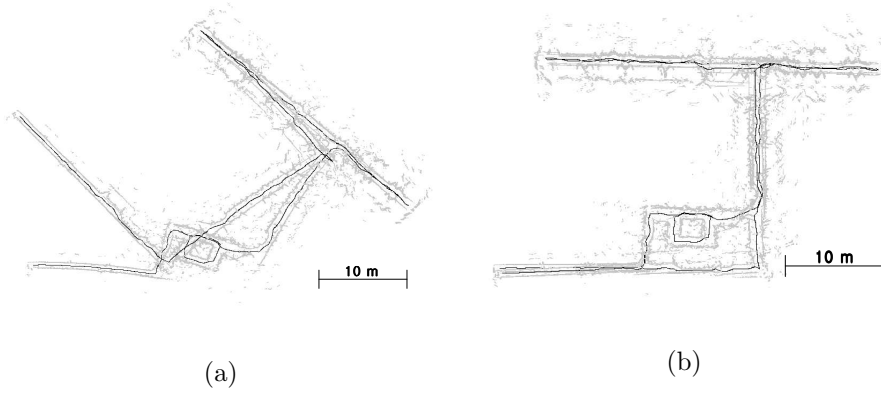


Figure 8: The constructed maps by the synchro-drive robot. (a) is an odometry map and (b) is a PC-method corrected map.

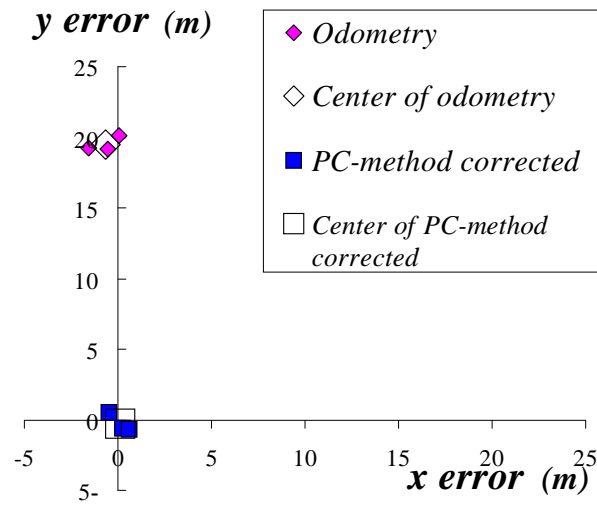


Figure 9: Endpoint errors after 177.2m of navigation with the synchro-drive robot.

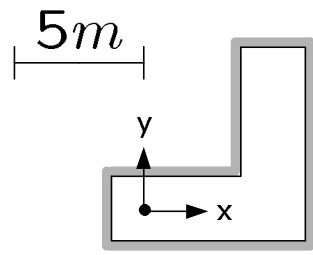
This experiment was repeated a total of three times. Endpoint errors, which are simply the final points estimated by the odometry because the real end point is the same as the real start point, were analyzed in Fig. 9. The average error of the raw odometry was  $19.52m$ , and that of the corrected odometry was  $0.28m$ , which is a 70.6 fold enhancement in this experiment. These results validate our assumption that the systematic errors are compensated for.

Once the systematic errors are removed, we can estimate the covariance matrix from the CFOP and CBOP. The variances of the non-systematic errors for  $\overline{\Delta D} = 1.45e^{-2}m$ ,  $\overline{\Delta \Theta} = 4.38e^{-3}rad$  were calculated by (3) as

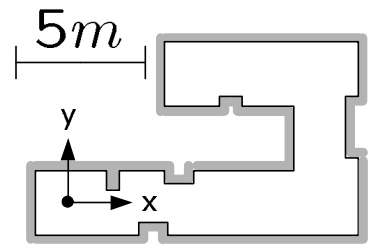
$$\begin{aligned}\sigma_{\Delta D}^2 &= 4.24e^{-6}m^2, \\ \sigma_{\Delta \Theta}^2 &= 7.97e^{-5}rad^2.\end{aligned}\tag{13}$$

To verify these variances, we ran the robot 100 times along 4 different paths (25 times per each path). The lengths of the paths were  $20m$ ,  $40m$ ,  $50m$  and  $80m$  as shown in Fig. 10. The velocity of the robot was set as  $0.13m/s$ , which is the same speed that was used for the FOP/BOP generation. We also ran the robot on the same floor used for the FOP/BOP generation.

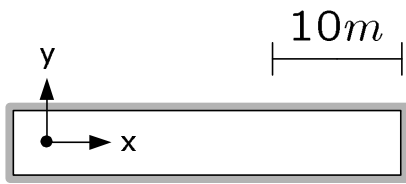
The probability density function (pdf) of the position uncertainty will have an arbitrary shape after various motions. However, let us assume the pdf to be the Gaussian distribution for validation purposes. Under this assumption,  $\sigma$ -bounds of the covariance matrices calculated by (12) are plotted in Fig. 11 for various path lengths. Note that the volume of the  $40m$  bound is relatively large because the  $40m$  path (Fig. 10(b)) has more detailed maneuvers than the others. These maneuvers increase  $\sigma_{\xi}(k)$  in (11) and



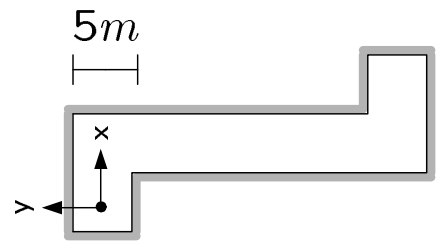
(a)



(b)



(c)



(d)

Figure 10: Four paths are navigated by the robot to verify the covariance matrix. The lengths of the paths are (a)  $20m$ , (b)  $40m$ , (c)  $50m$  and (d)  $80m$ . The robot started and ended at the center of the coordinate.

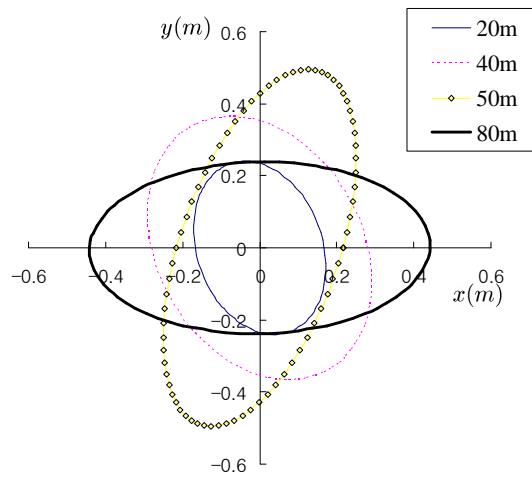


Figure 11:  $\sigma$ -bounds of the covariance matrices of the synchro-drive robot.

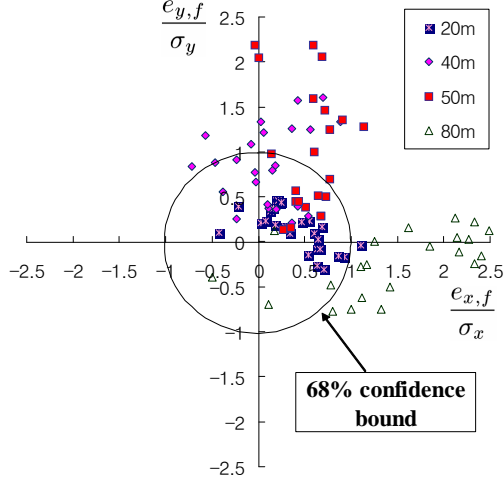


Figure 12: Data plot of  $\frac{e_{x,f}}{\sigma_x}$  versus  $\frac{e_{y,f}}{\sigma_y}$  of the synchro-drive robot.

expand the  $\sigma$ -bound. Also, note that the 50m and 80m bounds are stretched in the  $y$  and  $x$  directions, respectively. This reflects the real phenomenon that the  $\sigma$ -bound grows in a direction perpendicular to the heading angle of the robot.

To validate the accuracy of the covariance matrices,  $e_{x,f}$  and  $e_{y,f}$  are defined as

$$\begin{aligned} e_{x,f} &= x_f - \hat{x}_f, \\ e_{y,f} &= y_f - \hat{y}_f, \end{aligned} \tag{14}$$

where  $(x_f, y_f)$  and  $(\hat{x}_f, \hat{y}_f)$  are an actual final point and a final point estimated by the corrected odometry. For comparison, we normalized  $e_{x,f}$  and  $e_{y,f}$  over  $\sigma_x$  and  $\sigma_y$  and plotted 100 results in Fig. 12. The circle in Fig. 12 is the 68% confidence bound. In other words, the probability of  $\frac{e_{x,f}}{\sigma_x}$  and  $\frac{e_{y,f}}{\sigma_y}$  to be located within the unit circle is 68%. The experimental results show that the probability is 59%, which is 9% less than the ideal value. Therefore, we assert that the proposed method is capable of estimating the covariance matrix.

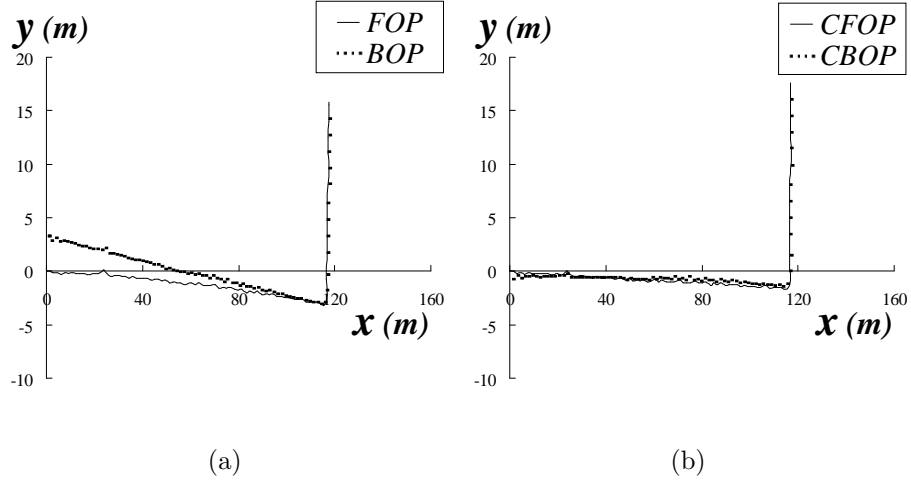


Figure 13: Forward and backward odometry paths for the error parameters estimation of the differential drive robot. (a) is the FOP/BOP and (b) is the CFOP/CBOP.

Two remarks should be made. First, the expectation values of  $e_{x,f}$  and  $e_{y,f}$  are not zero because there remain systematic errors that were not completely compensated for by the PC-method correction. Second, coefficients of the covariance matrix grow as the moving speed increases. In our experiments, we found out that the coefficient of the covariance matrix grows by 1.67 times at double speed of navigation.

## 5 Experiment 2: differential drive robot

The proposed method was also applied to a differential drive robot to validate the performance of the covariance matrix estimation. The robot was run along a GVG path whose length was 138m to get the FOP/BOP and the CFOP/CBOP as shown in Fig. 13.

To verify that that the systematic errors are compensated for, the robot was set to yield two sets of

odometry data. One is the raw odometry data and the other is the corrected odometry data. Then the robot, moving at  $0.25m/s$ , navigated  $719.1m$ , returning to the starting point. Two maps from the raw odometry and the corrected odometry are shown in Fig. 14.

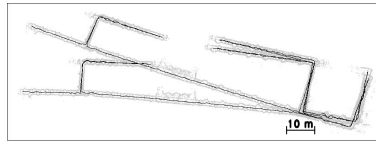
This experiment was repeated a total of three times. The endpoint errors were analyzed in Fig. 15. The average error of the raw odometry was  $25.7m$ , and that of the corrected odometry was  $4.4m$ , which is a 5.8 fold enhancement.

Once the systematic errors are removed, we can estimate the covariance matrix from the CFOP and CBOP. The variances of the non-systematic errors for  $\overline{\Delta D} = 1.45e^{-2}m$ ,  $\overline{\Delta \Theta} = 4.39e^{-3}rad$  were calculated by (4) as

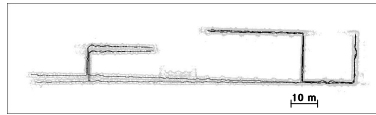
$$\begin{aligned}\sigma_{\Delta D}^2 &= 3.17e^{-6}m^2, \\ \sigma_{\Delta \Theta}^2 &= 1.07e^{-4}rad^2.\end{aligned}\tag{15}$$

To verify these variances, we ran the robot 100 times along the 4 different paths shown in Fig. 10. The velocity of the robot was set as  $0.25m/s$ , the same speed that was used for the FOP/BOP generation. Under the same Gaussian assumption as in Section 4,  $\sigma$ -bounds of the covariance matrices calculated by (12) are plotted in Fig. 16 for various path lengths. Like the phenomena of the synchro-drive robot, the volume of the  $40m$  bound is relatively large, and the  $50m, 80m$  bounds are stretched in  $y$  and  $x$  directions, respectively.

To validate the accuracy of the covariance matrices, we normalized  $e_{x,f}$ ,  $e_{y,f}$  over  $\sigma_x$ ,  $\sigma_y$  and plotted 100 results in Fig. 17. The circle in Fig. 17 is the 68% confidence bound. The experimental results showed



(a)



(b)

Figure 14: Maps constructed by the differential drive robot. (a) is an odometry map, and (b) is a PC-method corrected map.

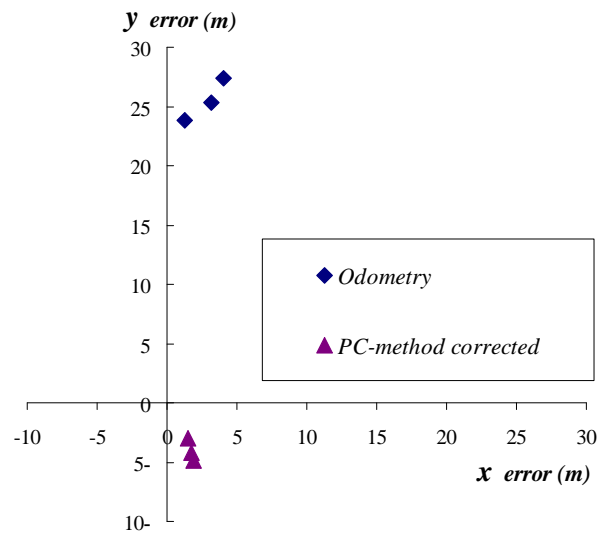


Figure 15: Endpoint errors after 719.1m of navigation with the differential drive robot.

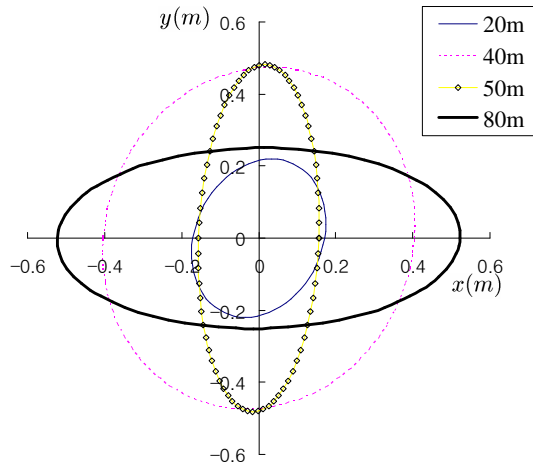


Figure 16:  $\sigma$ -bounds of the covariance matrices of the differential drive robot.

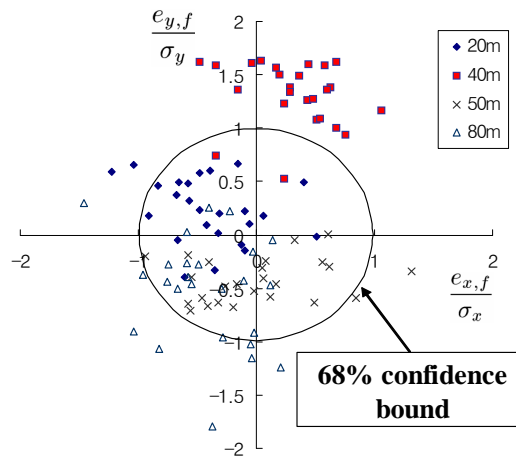


Figure 17: Data plot of  $\frac{e_{x,f}}{\sigma_x}$  versus  $\frac{e_{y,f}}{\sigma_y}$  of the differential drive robot.

that the probability of the  $\frac{e_{x,f}}{\sigma_x}, \frac{e_{y,f}}{\sigma_y}$  to be located within the unit circle was 68%, exactly the same as the ideal value. Although we are unable to argue that the covariance matrices are exact because the position uncertainty does not take the Gaussian form, it is verifiably clear that the proposed method can approximate the covariance matrix for differential drive robots.

## 6 Conclusion

This paper described a new method for an quantitative estimation of the covariance matrix which represents the uncertainty of the odometry induced by non-systematic errors. The proposed method is based on the idea that if a robot, whose systematic errors are fully compensated for, navigates the same path twice, the two odometry paths should coincide without the non-systematic errors. The proposed method predicted the non-systematic errors at the lowest level (*i.e.* the encoder level) so that the effects of the non-systematic errors can be extended into all mobile states such as the heading angle of the robot, the off-diagonal terms of the covariance matrix and so on.

Extensive experimental results showed that the covariance matrix estimated by the proposed method is accurate enough for practical uses (9 % offset from the ideal value for the synchro drive, and reasonably accurate for the differential drive robot).

## Appendix A

Let us assume that the initial covariance matrix  $P(0)$  is positive semi-definite. Then  $P(k)$  is positive semi-definite, if  $U(K)$  in (12) is positive semi-definite.

For simplicity, let us define

$$D \equiv \Delta D^2(k)$$

$$\alpha \equiv \sigma_{\Delta D}^2(k)$$

$$\beta \equiv \sigma_{\xi}^2(k)$$

$$A \equiv \sin \xi(k)$$

$$B \equiv \cos \xi(k).$$

Then, the matrix  $U(k)$  can be simply written as

$$U(k) = \begin{bmatrix} \sigma_{u_x}^2 & \sigma_{u_x u_y} \\ \sigma_{u_x u_y} & \sigma_{u_y}^2 \end{bmatrix} = \begin{bmatrix} D\beta A^2 + \alpha B^2 & (\alpha - D\beta)AB \\ (\alpha - D\beta)AB & D\beta B^2 + \alpha A^2 \end{bmatrix}.$$

The principal minors of  $U(k)$  are  $\sigma_{u_x}^2$  and  $\det(U(k))$ . Here  $\sigma_{u_x}^2 \geq 0$  and  $\det(U(k))$  is

$$\begin{aligned} \det(U(k)) &= (D\beta A^2 + \alpha B^2) \times (D\beta B^2 + \alpha A^2) - ((\alpha - D\beta)AB)^2 \\ &= D\alpha\beta(A^2 - B^2)^2 \geq 0. \end{aligned}$$

Thus  $U(k)$  is positive semi-definite because all principal minors are larger than zero. Therefore  $P(k)$  is positive semi-definite. ■

## REFERENCES

- [1] J. Borenstein and L. Feng, "Measurement and correction of systematic odometry errors in mobile robots," *IEEE Trans. on Robotics and Automation*, vol. 12, no. 6, pp. 869–880, 1996.
- [2] N. L. Doh, H. Choset, and W. K. Chung, "Accurate relative localization using odometry," in *International Conference on Robotics and Automation*, pp. 1606–1612, 2003.
- [3] S. Thrun, W. Burgard, and D. Fox, "A probabilistic approach to concurrent mapping and localization for mobile robots," *Machine Learning*, vol. 31, pp. 29–53, 1998.
- [4] C. M. Wang, "Location estimation and uncertainty analysis for mobile robots," in *International Conference on Robotics and Automation*, pp. 1230–1235, 1988.
- [5] K. S. Chong and L. Kleeman, "Accurate odometry and error modelling for a mobile robot," in *International Conference on Robotics and Automation*, pp. 2783–2788, 1997.
- [6] P. Goel, S. I. Roumeliotis, and G. S. Sukhatme, "Robust localization using relative and absolute position estimates," in *Proc. of IEEE/RSJ Int. Conf. on Intelligent Robots and Systems*, pp. 1134–1140, 1999.
- [7] K. S. Chong and L. Kleeman, "Mobile robot map building for an advanced sonar array and accurate odometry," *International Journal of Robotics Research*, vol. 18, no. 1, pp. 20–36, 1999.
- [8] O. Bengtsson and A. Baerveldt, "Localization in changing environment-estimation of a covariance matrix for the IDC algorithm," in *Proc. of IEEE/RSJ Int. Conf. on Intelligent Robots and Systems*, pp. 1931–1937, 2001.
- [9] A. Martinelli, N. Tomatis, A. Tapus, and R. Siegwart, "Simultaneous localization and odometry calibration for mobile robot," in *Proc. of IEEE/RSJ Int. Conf. on Intelligent Robots and Systems*, pp. 1499–1504, 2003.
- [10] A. Kelly, "Linearized error propagation in odometry," *International Journal of Robotics Research*, vol. 23, no. 2, pp. 179–218, 2004.
- [11] N. L. Doh, W. K. Chung, and Y. Youm, "A covariance matrix estimation method for position uncertainty of the wheeled mobile robot," in *International Conference on Control, Automation and Systems*, pp. 1933–1938, 2003.
- [12] H. Choset and K. Nagatani, "Topological SLAM: Toward exact localization without explicit localization," *IEEE Trans. on Robotics and Automation*, pp. 125–137, 2001.
- [13] D. Lerro and Y. Bar-Shalom, "Tracking with debiased consistent converted measurements versus EKF," *IEEE Trans. on Aerospace and Electronic Systems*, vol. 29, no. 3, pp. 1015–1022, 1993.

## List of captions

1. If a robot follows a straight line, an error bound of odometry will look like a banana as in (a). To approximate this banana shape, researchers have used a covariance matrix whose ellipse covers the banana shape as in (b).
2. A robot moved a straight line rotated by  $45^\circ$ . The real error bound, then, will be like the dotted ellipse but our previous method will yield an overestimated error bound whose axes are aligned with the world coordinate.
3. Schematic explanation of the PC-method. (a) is a plot before correction and (b) is a plot after correction.
4. Method of approximating the non-systematic errors: (a) The CFOP/CBOP do not perfectly overlap even after the systematic error compensation. (b)  $\epsilon_{(\cdot)}(1)$  can be found which changes the first CBOP point into its matching CFOP point. This procedure can be applied to succeeding matching pairs as in (c) and (d).
5. Typical shape of rugged environments.
6. Large uncompensated systematic errors affect the CFOP and CBOP strongly.
7. Forward and backward odometry paths for the error parameters estimation of the synchro-drive robot. (a) is the FOP/BOP and (b) is the CFOP/CBOP.

8. The constructed maps by the synchro-drive robot. (a) is an odometry map and (b) is a PC-method corrected map.
9. Endpoint errors after 177.2m of navigation with the synchro-drive robot.
10. Four paths are navigated by the robot to verify the covariance matrix. The lengths of the paths are (a) 20m, (b) 40m, (c) 50m and (d) 80m. The robot started and ended at the center of the coordinate.
11.  $\sigma$ -bounds of the covariance matrices of the synchro-drive robot.
12. Data plot of  $\frac{e_{x,f}}{\sigma_x}$  versus  $\frac{e_{y,f}}{\sigma_y}$  of the synchro-drive robot.
13. Forward and backward odometry paths for the error parameters estimation of the differential drive robot. (a) is the FOP/BOP and (b) is the CFOP/CBOP.
14. Maps constructed by the differential drive robot. (a) is an odometry map, and (b) is a PC-method corrected map.
15. Endpoint errors after 719.1m of navigation with the differential drive robot.
16.  $\sigma$ -bounds of the covariance matrices of the differential drive robot.
17. Data plot of  $\frac{e_{x,f}}{\sigma_x}$  versus  $\frac{e_{y,f}}{\sigma_y}$  of the differential drive robot.